Magnetic linear dichroism in electron energy loss spectroscopy

J. Yuan and N. K. Menon
Department of Physics, Cavendish Laboratory, Madingley Road, Cambridge CB3 OHE, United Kingdom

In this article, we demonstrate the effect of magnetic linear dichroism (MLD) in electron energy loss spectroscopy (EELS), as applied to the antiferromagnetic compound α-Fe_2O_3. The experiments were performed in a high resolution scanning transmission electron microscope (STEM), capable of producing a nanoscale electron probe. The resultant difference spectrum is consistent with the MLD observed in x-ray absorption spectroscopy and the known magnetic structure of Hematite, suggesting that MLD in EELS, coupled with the high spatial resolution attainable in STEM, is a useful technique in the study of magnetic microstructure. © *1997 American Institute of Physics.* [S0021-8979(97)61108-1]

I. INTRODUCTION

The study of microstructural magnetism is, at present, possible using a number of techniques that can be broadly classified into those relying on elastic scattering processes and those which are spectroscopy based. Magnetic domain structure has long been studied by Lorentz microscopy,[1] and this provides an example of the former technique. Recently, spectroscopic techniques have become widely available with the abundance of polarized photons from modern synchrotron sources. Those involving core electron excitation have the advantage of chemical specificity. Electron energy loss spectroscopy (EELS) measures the probability that a high energy electron loses a quantum of energy when it interacts with a material. The resulting spectrum provides valuable chemical and structural information. It has been well documented[2] to be analogous in many ways to x-ray absorption spectroscopy but, with the added advantages of high spatial resolution associated with focused electrons, the experiment can be conducted in a laboratory environment. In this article, we demonstrate the feasibility of observing magnetic linear dichroism in EELS, as applied to the compound α-Fe_2O_3.

II. TECHNICAL BACKGROUND

In x-ray absorption spectroscopy of magnetic materials, attention has thus far focused on magnetic circular dichroism (MCD), defined to be the difference in absorption cross section for left and right polarization. This difference is proportional to the average value of the magnetization $\langle \mathbf{M} \rangle$, and is therefore zero for antiferromagnetic materials. Using linearly polarized photons, one can study magnetic linear dichroism (MLD), which is defined to be the difference in absorption cross section for incident electric fields polarized parallel and perpendicular to the magnetization in the material. It depends on $\langle M^2 \rangle$ of the ions in the solid,[3,4] and can therefore be strong in any system with collinear magnetic ordering.

In EELS, energy losses are due to the interaction of the field of the fast incident electrons with the atoms in the solid. It can be shown[6] that the perturbing field due to the incident electron beam, $\mathbf{E}(\mathbf{r},t)$, can be decomposed in Fourier space into a superposition of components of the form

$$\mathbf{E}(\mathbf{q},\omega) \approx i\phi(\mathbf{q},\omega)\mathbf{q}, \tag{1}$$

where $i = \sqrt{-1}$, $\mathbf{q}(=\mathbf{k_i}-\mathbf{k_f})$ is the momentum transfer and ϕ is a scalar function of $\mathbf{q}$ and ω. It can be seen that these component waves are longitudinally polarized parallel to the direction of momentum transfer, $\mathbf{q}$ (see Fig. 1 below), and hence being only capable of linear polarization. The control of their polarization direction relative to the magnetization $\mathbf{M}$ makes it possible to observe MLD. In this analysis, we have assumed that the fast electron trajectory is hardly affected by the energy loss process. This is the so-called small-angle approximation satisfied in the high energy setup described below. An attempt has been made to observe MCD in EELS[5] involving rarer large-angle inelastic scattering, though without definite conclusions yet.

We chose to consider the compound hematite (α-Fe_2O_3), whose magnetic and crystal structure is well known.[7] The crystal structure of hematite is trigonal, with $a=b=0.5038$ nm and $c=1.3772$ nm. There are six formula units per unit cell, combining to yield the uniaxial corundum structure in which the iron atoms are coordinated by six oxygen atoms with slight deviations from octahedral (O_h) symmetry.

Hematite has an antiferromagnetic ground state, with spins on specific neighboring planes oriented in opposite directions, implying that the magnetization $\langle \mathbf{M} \rangle = 0$. Neutron diffraction studies of the spin structure[7,8] have shown that, above a certain temperature, known as the Morin temperature $T_m (\sim -10\ ^\circ\mathrm{C})$, the moments are aligned perpendicular to the c axis of the crystal, and are always parallel within any basal plane. In addition, neighboring basal planes are antiferromagnetically coupled. At temperatures below T_m, a magnetic phase transition takes place which results in the orientation of the magnetic moments switching by 90°. The spins are then parallel to the c axis. The layered structure of the

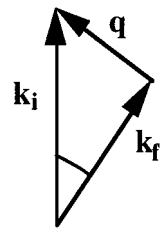

FIG. 1. Scattering geometry for EELS. The terms $\mathbf{k_i}$ and $\mathbf{k_f}$ denote the initial and final wave vectors of the fast electron. The term $\mathbf{q}$ is the momentum transfer.

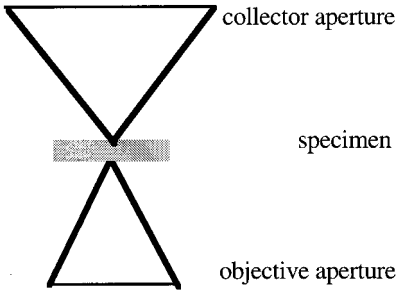

FIG. 2. The configuration of STEM for high resolution imaging. The objective and collector apertures control the range of the incident and scattered wave vectors.

ordered spins in this material provides a good model system to study MLD.

III. EXPERIMENTAL DETAILS

The experiments were carried out in a dedicated VG-HB501 scanning transmission electron microscope (STEM) with a charge coupled device (CCD) based parallel EELS detector at Cambridge. The anatomy of the microscope[9] is such that a sub-nanometer-sized electron probe can be produced at the specimen, thus yielding a high spatial resolution that makes the STEM an ideal environment for probing microstructure.

The measurements were conducted on a small crystallite sample of hematite at room temperature. The orientation of the crystallites relative to the incident beam was adjusted in order to align the c axis with the incident beam direction. This was done by observing the diffraction pattern and tilting the specimen until the characteristic hexagonal symmetry is observed. The magnetization $\mathbf{M}$ is then perpendicular to the microscope axis. The thickness of the specimen analyzed is typically less than 500 Å, as estimated from the plasmon excitation probability. The spatial resolution of the EELS signal is determined by the probe size at the specimen and the detector size at this thin film limit.

It can be seen from Eq. (1) that the control of the electric field orientation can be achieved by sampling different $\mathbf{q}$ vectors. However, the high spatial resolution of 1–2 nm is achieved using an electron probe containing a range of incident electron wave vectors $\mathbf{k_i}$ (typically spanning 3–8 mrad convergence semiangle). The detector also sustains a finite solid angle, allowing electrons with a range of final wave vectors $\mathbf{k_f}$ (typically spanning up to 7 mrad collection semiangle). Thus, the resulting EELS always contains a range of $\mathbf{q}$ vectors. If we decompose $\mathbf{q}$ into a component perpendicular to $\mathbf{k_i}(\mathbf{q}_\perp)$ and one that is parallel to $\mathbf{k_i}(\mathbf{q}_\parallel)$, the dichroic information can still be obtained if we can collect two different spectra containing a varying weighting of the contributions from the two $\mathbf{q}$ components.[10] In this case, we achieve this by varying the convergence angle of the incident electrons.

We chose to consider the $L_{2,3}$ absorption of the Fe^{3+} ion in hematite, with the dominant excitation being $2p^6 3d^0 \rightarrow 2p^5 3d^1$, as it was expected that the dichroic effects are maximized in this case. In Fig. 3, we have shown two spectra

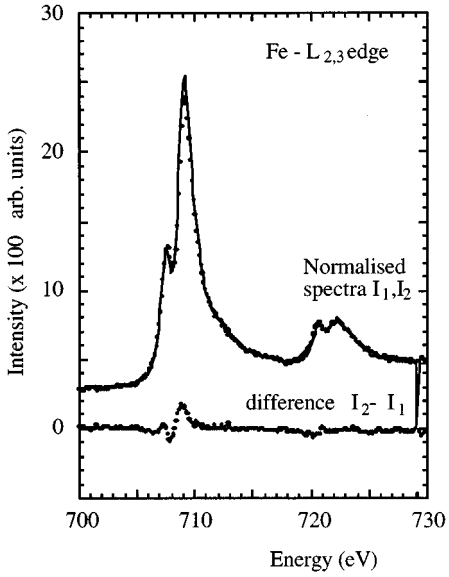

FIG. 3. Normalized EELS spectra of Fe $2p$ absorption in hematite obtained using 25 μm (I_1—dotted line) and 50 μm (I_2—solid line) objective apertures. Also plotted is the difference (I_2-I_1) which is proportional to the magnetic dichroism effect.

acquired for objective aperture sizes of 25 and 50 μm, corresponding to convergence angles of 3.5 and 7.0 mrad, respectively, for 100 keV incident electrons. The spectra consist of two groups of peaks, corresponding approximately to transition from the spin-orbit split Fe's $2p$ core hole states to the crystal field split $3d$ states. The dichroic effect manifests itself as the small intensity difference in the fine structure within the main peaks. Since they are quite small, a large acquisition time of 20 s per single acquisition was required to collect the weak core loss signal. A larger acquisition time is not possible because of the presence of energy and specimen drifts. Further improvements to the signal-to-noise ratio are achieved by aligning and summing many similar spectra. No sign of radiation damage is observed.

The spectra collected with the larger 50 μm aperture will contain more contribution from $\mathbf{q}_\perp$ components that from the spectra collected with the 25 μm aperture. To quantify the difference spectra, we may denote I_1 and I_2 to be the normalized spectral intensities detected for each of the objective apertures. The normalization is carried out so that the isotropic part of the spectra (i.e., the pre-edge intensities) are equalized. The normalized intensity can be written as $I_1=\alpha_1 I_\parallel+\beta_1 I_\perp$; $I_2=\alpha_2 I_\parallel+\beta_2 I_\perp$, where $I_\parallel$ and $I_\perp$ are the intensities for incident field polarizations parallel and perpendicular to $\mathbf{k_i}$. The normalization constraint is then $\alpha_1+\beta_1=\alpha_2+\beta_2$. In this case, the difference spectrum is then given by

$$I_{\text{diff}}=I_2-I_1=(\alpha_2-\alpha_1)(I_\parallel-I_\perp). \tag{2}$$

It can be seen from Eq. (2) that the detected difference in intensity is thus proportional to the difference in cross section for field polarizations parallel and perpendicular to the spin of the ions in the solid. The processed difference spectrum for hematite is also shown in Fig. 3. It has a peak intensity that is approximately 5% of the acquired spectra.

IV. DISCUSSION

The dichroism effect in solids can normally be attributed to either (or both) the anisotropic crystal field due to the array of oxygen anions surrounding the relevant cation or a local magnetic field **B** produced, for example, as a result of the next to nearest neighbor superexchange interaction, both of which result in a splitting of the J levels. The different dipole selection rules for polarization parallel ($\Delta M_J=0$) and perpendicular ($\Delta M_J=\pm 1$) to the anisotropic axis make transitions to final states with $J'=J-1,J,J+1$ have different intensities. Dichroic spectra collected on either side of the Morin transition temperature suggest that the local exchange field due to ordered spins has the dominant effect in MLD of the Fe's $2p$ absorption spectra.[14] In this case, the sign of the difference spectra shown in Fig. 3 is consistent with the ordered spin oriented perpendicular to the beam direction. With the specimen c axis aligned with the beam direction, we conclude that the spin is in the basal plane despite the presence of the longitudinal magnetic field in the pole piece of the STEM microscope. It is understandable because the longitudinal field inside a STEM is only 1–2 T and is much smaller than the local exchange field.[11]

The above consideration assumed a dipole induced transition, which arises due to an expansion of the transition matrix element in Fermi's golden rule. The matrix element can be shown to take the form[12]

$$M_{\mathrm{fi}} \propto \frac{1}{q^2} \langle \phi_f | e^{\mathbf{iqr_i}} | \phi_i \rangle, \tag{3}$$

where ϕ_f and ϕ_i are the final and initial atomic wave functions, and $\mathbf{r_i}$ are the coordinates of the atomic electron of interest. The dipole term arises from the first order ($\mathbf{iq \cdot ri}$) expansion of the exponential factor, and will dominate for small **q**. The second order term could be of considerable importance for larger values of **q**, and this might influence the interpretation of the difference spectrum. However, it is known that for quadrupolar transitions to take place, the parity of the initial and final wave functions must be the same. This is not the case for the transition $2p^6 3d^0 \rightarrow 2p^5 3d^1$ (which is the dominant excitation in the energy range of interest), and therefore we concluded that quadrupole effects are unimportant in the interpretation of the difference spectra.

So far, we have neglected the relativistic effects which might also be important, as the incident electron beam is accelerated through 100 kV, acquiring a speed of ~0.5 c. It has been demonstrated,[13] however, that the numerical modification is negligibly small.

V. CONCLUSION

We have demonstrated the phenomenon of the magnetic linear dichroism in electron energy loss spectroscopy, as applied to the antiferromagnetic compound α-Fe_2O_3. The form of the difference spectrum is consistent with similar observations made using x-ray absorption spectroscopy.[14] Since significant effects are observed with a nanosized focused electron probe, this opens the way for high resolution study of micromagnetism in thin films with chemical specificity. It will thus be complementary to the more conventional high resolution techniques such as Lorentz microscopy or holography.

ACKNOWLEDGMENTS

This work was supported by the Engineering and Physical Sciences Research Council, UK.

[1] P. B. Hirsch, A. Howie, R. B. Nicholson, D. W. Pashley, and M. J. Whelan, *Electron Microscopy of Thin Crystals* (Butterworths, London, 1965).
[2] A. P. Hitchcock, Jpn. J. Appl. Phys. 1 **32**, 176 (1993).
[3] G. van der Laan, B. T. Thole, G. A. Sawatzky, J. B. Goedkoop, J. C. Fuggle, J. M. Esteva, R. Karnatak, J. P. Remeika, and H. A. Dabkowska, Phys. Rev. B **34**, 6529 (1986).
[4] B. T. Thole, G. van der Laan, and G. A. Sawatzky, Phys. Rev. Lett. **55**, 2086 (1985).
[5] G. R. Harp, R. F. C. Farrow, and R. F. Marks, J. Appl. Phys. **79**, 6496 (1995).
[6] J. D. Jackson, *Classical Electrodynamics* (Wiley, New York, 1976).
[7] C. G. Shull, W. A. Strauser, and E. O. Wollan, Phys. Rev. **83**, 333 (1951).
[8] R. Nathans, S. J. Pickart, H. A. Alperin, and P. J. Brown, Phys. Rev. **136**, 1641 (1964).
[9] C. Colliex and C. Mory, in *Quantitative Electron Microscopy*, edited by J. N. Chapman (SUSSP, Edinburgh, 1983).
[10] N. D. Browning, J. Yuan, and L. M. Brown, Philos. Mag. A 261 (1993).
[11] A. P. Morrish, *Canted Antiferromagnetism: Hematite* (World Scientific, Singapore, 1995).
[12] M. Inokuti, Rev. Mod. Phys. **43**, 297 (1971).
[13] R. F. Egerton, *Electron Energy Loss Spectroscopy in the Electron Microscope* (Plenum, New York, 1986).
[14] P. Kuiper, B. G. Searle, P. Rudolf, L. H. Tjeng, and C. T. Chen, Phys. Rev. Lett. **70**, 1549 (1993).